

## A finite element approach for the analysis of active slow-moving landslides

**Abstract** In the present paper, a finite element approach is proposed to analyse the mobility of active landslides which are controlled by groundwater fluctuations within the slope. These landslides are usually characterised by low displacement rates with deformations that are essentially concentrated within a narrow shear zone above which the unstable soil mass moves with deformations of no great concern. The proposed approach utilises an elasto-viscoplastic constitutive model in conjunction with a Mohr-Coulomb yield function to describe the behaviour of the soil in the shear zone. For the other soils involved by the landslide, an elastic model is used for the sake of simplicity. A significant advantage of the present method lies in the fact that few constitutive parameters are required as input data, the most of which can be readily obtained by conventional geotechnical tests. The rest of the required parameters should be calibrated on the basis of the available monitoring data concerning the change in the piezometric levels and the associated movements of the unstable soil mass. After being calibrated and validated, the proposed approach can be used to predict future landslide movements owing to expected groundwater fluctuations or to assess the effectiveness of drainage systems which are designed to control the landslide mobility. The method is applied to back-predict the observed field behaviour of three active slow-moving landslides documented in the literature.

**Keywords** Active landslide · Groundwater fluctuation · Landslide mobility · Finite element method · Viscous behaviour

### Introduction

Active landslides which are controlled by groundwater fluctuations generally occur in gentle slopes of clayey soils. The main type of movement experienced by these landslides is a translational or roto-translational slide with a velocity of order of a few centimetres per year. Therefore, they can be classified as very slow or extremely slow landslides, according to Cruden and Varnes (1996). Typically, deformations are concentrated within a shear zone located at the base of the landslide body, in which the soil shear strength is at residual condition owing to the high level of accumulated strain (Leroueil et al. 1996). The landslide body on the contrary experiences very small strains. Generally, the slope movements are caused by an increase in pore water pressure with the total stress field that remains practically unchanged with movement. For saturated soils, this increase in pore pressure determines a decrease in effective stress and consequently in the soil shear strength along the slip surface. Considering that the slope safety factor,  $SF$ , is governed by the residual strength along the slip surface; the values of  $SF$  are generally low. Therefore, small changes in pore pressure can produce significant changes in the displacement rate of the unstable soil mass. These changes are often caused by groundwater level fluctuations which in turn are related to rainfall. Therefore, the mobility of these landslides is characterised by alternating phases of rest and reactivation in accordance with the seasonal rainfall conditions. In particular, a

rising groundwater level causes a reactivation and subsequent acceleration of the landslide because the resisting force decreases and cannot balance the destabilising force. On the other hand, a groundwater level reduction (as it occurs during dry periods) attenuates the landslide velocity and may eventually bring the soil mass to rest. In addition, in the portion of soil under unsaturated condition, a reduction in suction owing to rainwater infiltration in the wet periods reduces the shear strength of the soil, which in turn reduces the slope stability. On the contrary, evaporation of moisture within the soil in dry periods results in an increase of suction with consequent increase in soil shear strength and slope stability (Fredlund and Rahardjo 1993). The continuous reactivation phases can cause significant damage to the structures and infrastructures located on the slope. Therefore, an adequate consideration of these phenomena is necessary for performing realistic slope stability analyses.

In the current applications, groundwater pressure regime and slope stability are usually dealt with in an uncoupled manner using some theoretical approaches. Specifically, the differential equations governing pore pressure changes within the slope due to changes in hydraulic conditions at the boundary are first solved. Then, the pore pressures calculated at the potential failure surface are used in a limit equilibrium analysis for assessing slope stability. In this connection, Conte and Troncone (2012a) proposed a simplified method that utilises the infinite slope model to assess slope stability and an analytical solution (Conte and Troncone 2008) to evaluate the changes in pore pressure at the slip surface from the pore pressure measurements at a piezometer which is installed above this surface. However, the limit equilibrium method is in principle unable to analyse active landslides for which a realistic prediction of the slope movements is required rather than a calculation of the safety factor. Calvello et al. (2008) proposed a numerical procedure in which the changes in pore pressure are first calculated by a physically based analysis. Then, the displacement rate at selected points is related empirically to the changes in the safety factor with time. These changes are evaluated by the limit equilibrium method on the basis of the changes in pore pressure calculated in the previous step.

Simplified methods were also developed to perform directly an approximate assessment of the landslide velocity (Angeli et al. 1996; Gottardi and Butterfield 2001; Corominas et al. 2005; Maugeri et al. 2006; Herrera et al. 2009; Conte and Troncone 2011, 2012b). In these methods, it is assumed that the landslide body behaves as a rigid block sliding on an inclined plane. The model is similar to that originally proposed by Newmark (1965) for predicting the earthquake-induced permanent displacements of slopes. Unlike this latter model, however, it is assumed that a viscous force is activated when motion of the unstable soil starts. This additional resisting force is applied at the base of the sliding soil mass and should account for, in an approximate manner, the effect of energy dissipation owing to the permanent strains occurring in the shear zone.

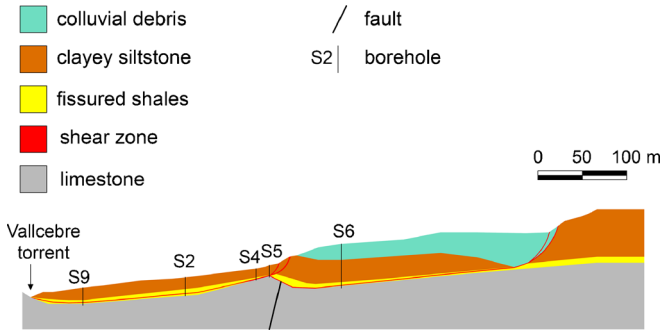


**Fig. 1** A geological cross-section of the Vallcebre landslide with an indication of the boreholes which were equipped by open standpipe piezometers (modified after Corominas et al. 2005). The scale is applicable to vertical and horizontal directions

Numerical models based on the finite element method or the finite difference method, in which reliable constitutive laws are incorporated, can obviously provide a better understanding of the complex mechanisms of deformation and failure that occur in the slope (Lollino et al. 2010). Considering that in slow-moving landslides the slope movements are essentially of viscous nature (Savage and Chleborad 1982; Vulliet and Hutter 1988; Van Asch and Van Genuchten 1990; Bracegirdle et al. 1992; Desai et al. (1995) developed a finite element approach for the analysis of natural slopes that exhibit slow and continuous movements under gravity load (creeping slopes). In this approach, an elasto-viscoplastic constitutive model is included to predict the behaviour of both the unstable soil mass and the soil in a finite “interface zone” located between the moving mass and the underlying stable geological formation. A similar constitutive model was also implemented in the finite element program Code\_Bright (Olivella et al. 1996; Ledesma et al. 2009). Picarelli et al. (2004) used the

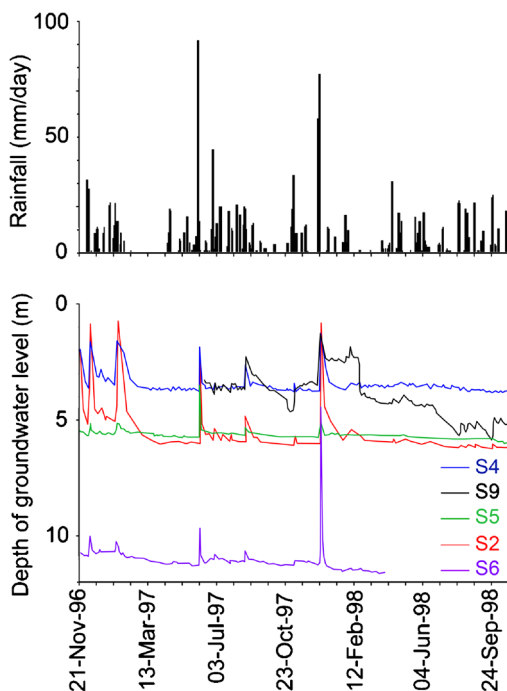


**Fig. 2** Rainfall and groundwater level measurements at Vallcebre (modified after Corominas et al. 2005)

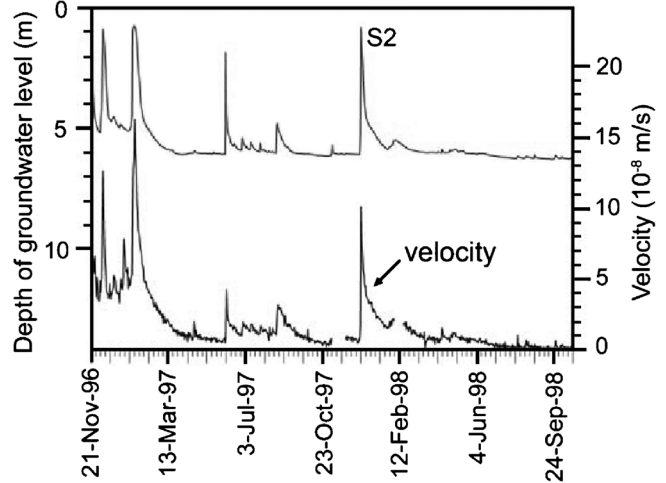


**Fig. 3** Piezometric levels and landslide velocity measured at borehole S2 from November 1996 to October 1998 (modified after Corominas et al. 2005)

constitutive law by Singh and Mitchel (1969) to describe the viscous behaviour of the landslide body, and elasto-plastic interface elements to simulate the slip surface. Therefore, no viscous displacement occurs along this slip surface.

A different finite element approach is proposed in the present paper for evaluating slow-moving landslide mobility owing to groundwater level fluctuations. This approach utilises an elasto-viscoplastic constitutive model in conjunction with a Mohr-Coulomb yield function to model the behaviour of the soil in the shear zone where the landslide displacement occurs. A linear elastic model is on the contrary considered for the other soils involved by the landslide. A significant advantage of the present method lies in the fact that few constitutive parameters are required as input data and that most of these parameters can be readily obtained by conventional geotechnical tests. The proposed approach is applied to analyse the mobility of three active landslides documented in the literature.

**Elasto-viscoplastic model**

Assuming small strains, the total strain rate tensor  $\dot{\epsilon}_{ij}$  for an elasto-viscoplastic material can be additively decomposed into an elastic component  $\dot{\epsilon}_{ij}^{el}$  and a viscoplastic component  $\dot{\epsilon}_{ij}^{vp}$  as follows

$$\dot{\epsilon}_{ij} = \dot{\epsilon}_{ij}^{el} + \dot{\epsilon}_{ij}^{vp} \tag{1}$$

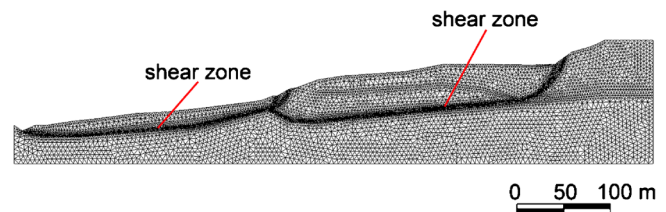


**Fig. 4** Finite element mesh used for the analysis of the Vallcebre landslide. The scale is applicable to the vertical and horizontal directions

**Table 1** Calibrated values of the soil parameters for the Vallcebre landslide

Material	$\gamma$ (kN/m <sup>3</sup> )	$E'$ (MPa)	$\nu'$	$\phi_r$ (°)	$\bar{\gamma}$ (1/day)	$k$ (m/day)
Colluvial debris	20.5	15	0.33			$9 \cdot 10^{-5}$
Clayey siltstone	20.5	15	0.40			$9 \cdot 10^{-6}$
Fissured shales	21.5	10	0.40			$9 \cdot 10^{-5}$
Shear zone	21.5	10	0.40	7.8–14.7	$4.5 \cdot 10^{-7}$	$9 \cdot 10^{-5}$
Limestone	22.0	100	0.40			$9 \cdot 10^{-7}$

The tensor  $\dot{\epsilon}_{ij}^{el}$  is defined as

$$\dot{\epsilon}_{ij}^{el} = C_{ijhk}^{el} \dot{\sigma}'_{hk} \quad (2)$$

where  $\dot{\sigma}'_{hk}$  is the effective stress rate tensor and  $C_{ijhk}^{el}$  is the elastic compliance tensor that is time-independent. Following Perzyna (1963), the viscoplastic strain rate tensor is expressed by the following equation:

$$\dot{\epsilon}_{ij}^{vp} = \Phi(F) m_{ij} \quad (4)$$

where  $\Phi$  is the viscous nucleus that depends on the yield function  $F$ , and  $m_{ij}$  is the gradient to the plastic potential function  $Q$  (i.e.  $m_{ij} = \partial Q / \partial \sigma'_{ij}$ ). The gradient of  $Q$  defines the direction of the viscoplastic strain rate tensor, and the yield function influences the modulus of this tensor by means of  $\Phi$ . The choice of the viscous nucleus  $\Phi$  is crucial for describing reliably the time-dependent behaviour of the material. In this connection, di Prisco and Imposimato (2002, 2003) proposed the following relationship for  $\Phi$ :

$$\Phi(F, p') = \bar{\gamma} p' e^{\bar{\alpha} F} \quad (5)$$

where  $\bar{\gamma}$  and  $\bar{\alpha}$  are constitutive parameters and  $p'$  is the mean effective stress. This equation is simple to implement in a finite element code and is capable to reproduce successfully experimental evidence (di Prisco and Imposimato 1996). In addition, using

Eq. 4 in conjunction with Eq. 5 allows the occurrence of viscoplastic strains at constant effective stress to be effectively simulated. The parameter  $\bar{\gamma}$  strongly influences the strain rate and consequently the rapidity with which strain occurs owing to a given stress increment. In particular, strain rate increases with increasing the value of  $\bar{\gamma}$ . The values of  $\bar{\alpha}$  and  $\bar{\gamma}$  are generally determined by matching the experimental results from specific creep tests with those obtained simulating numerically these tests. Considering that the viscous parameters from laboratory tests can significantly differ from those obtained from back-analysis of observed landslide velocity (Van Asch et al. 2007), in the present study, the value of  $\bar{\gamma}$  is back-calculated on the basis of field measurements of the displacements experienced by the landslide body, whereas a constant value of  $\bar{\alpha} = 61$  (di Prisco and Imposimato 1996; Troncone 2005; Conte et al. 2010) is assumed in all the analyses performed for the sake of simplicity. In addition, following di Prisco and Imposimato (1996, 2002), a maximum value of 3 is imposed to the product  $\bar{\alpha} F$  to prevent the exponent in Eq. 5 from becoming excessively large. In other words, in this study, it is assumed that the viscous behaviour of the soil is essentially controlled by the parameter  $\bar{\gamma}$ .

The Mohr-Coulomb failure criterion is adopted for defining the yield function  $F$ . The expression of  $F$  in terms of the principal effective stresses is

$$F = \frac{1}{2} (\sigma'_1 - \sigma'_3) - \frac{1}{2} (\sigma'_1 + \sigma'_3) \sin \phi' - c' \cos \phi' \quad (6)$$

where  $\sigma'_1$  and  $\sigma'_3$  are the major and minor principal effective stresses, respectively (it is assumed that compressive stress is positive),  $c'$  is the effective cohesion, and  $\phi'$  is the angle of the shearing resistance of the soil.

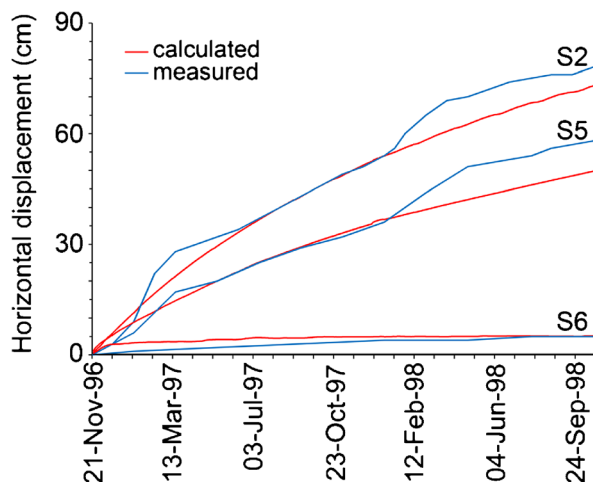


**Fig. 5** Vallcebre landslide: measured and calculated horizontal displacements versus time (modified after Corominas et al. 2005)

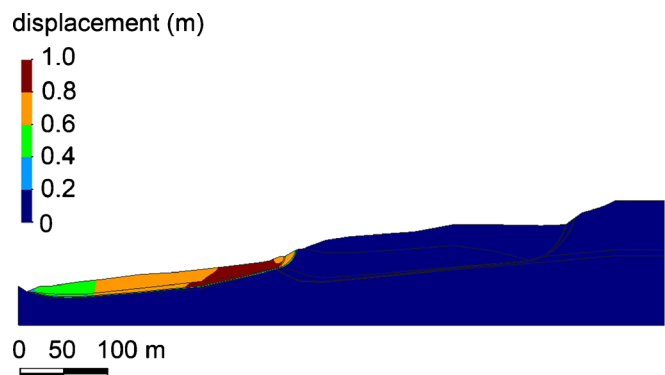


**Fig. 6** Vallcebre landslide: total displacement field calculated at the final time of analysis. The scale is applicable to the vertical and horizontal directions

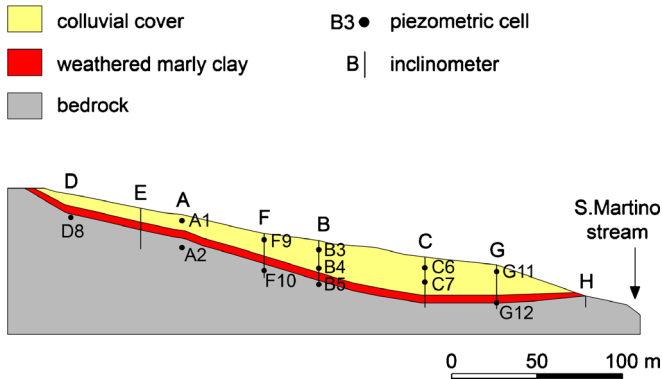


**Fig. 7** A geological cross-section at Fosso San Martino (modified after D’Elia et al. 1998). The scale is applicable to the vertical and horizontal directions

The flow rule is of non-associated type with the plastic potential function expressed as

$$Q = \frac{1}{2} (\sigma'_1 - \sigma'_3) - \frac{1}{2} (\sigma'_1 + \sigma'_3) \sin \psi \quad (7)$$

in which  $\psi$  is the dilatancy angle of the soil.

It is worthy to note that, for the soil in the shear zone,  $\phi'$  is replaced by the friction angle at residual,  $\phi'_r$ ,  $c'$  is generally negligible and  $\psi$  is nil. The described constitutive model therefore requires few soil parameters as input data, most of which can be readily obtained by conventional geotechnical tests. Specifically, the required parameters are Young’s modulus  $E'$ , Poisson’s ratio  $\nu'$ , the residual friction angle,  $\phi'_r$ , and the viscous parameters  $\bar{\alpha}$  and  $\bar{\gamma}$ . This is a significant advantage of the present model, especially when there is a lack of specific experimental data. In these circumstances, in fact, the use of more sophisticated constitutive models which involve a great number of parameters could not be fully justified.

**Analysis of case studies**

Three case studies are analysed: the Vallcebre landslide in Spain (Corominas et al. 2005), the Fosso San Martino landslide in Italy (Bertini et al. 1984) and the Steinernase landslide in Switzerland (Laloui et al. 2009). The primary objective of this analysis is to assess the capability of the proposed approach of capturing the main features of the landslide kinematics and obtaining representative values of some constitutive parameters (in particular, the viscous parameter  $\bar{\gamma}$ ) the evaluation of which is not generally a simple operation.

The selected landslides are active landslides that involve clayey soils and move with different velocity. Movements are controlled

**Table 2** Soil parameters obtained from laboratory and field tests by Bertini et al. (1984)

Material	$\gamma$ (kN/m <sup>3</sup> )	$\phi'_r$ (°)	$k_x$ (m/day)	$k_y$ (m/day)
Colluvial cover	21–22		0.05	
Weathered marly clay	19.9–21.5	17–22	0.05	
Bedrock	21.5–22.5		0.3–10	0.01–1

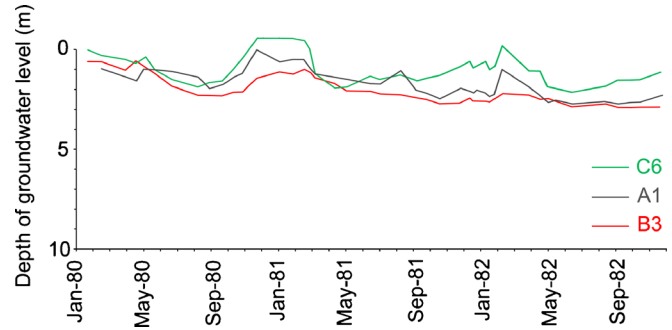


**Fig. 8** Piezometric measurements at Fosso San Martino (modified after Bertini et al. 1984)

by groundwater level fluctuations, and deformations are essentially concentrated in distinct shear zones. In addition, in all these landslides, an evident synchronism was observed between groundwater fluctuations and displacement rate. In other words, the

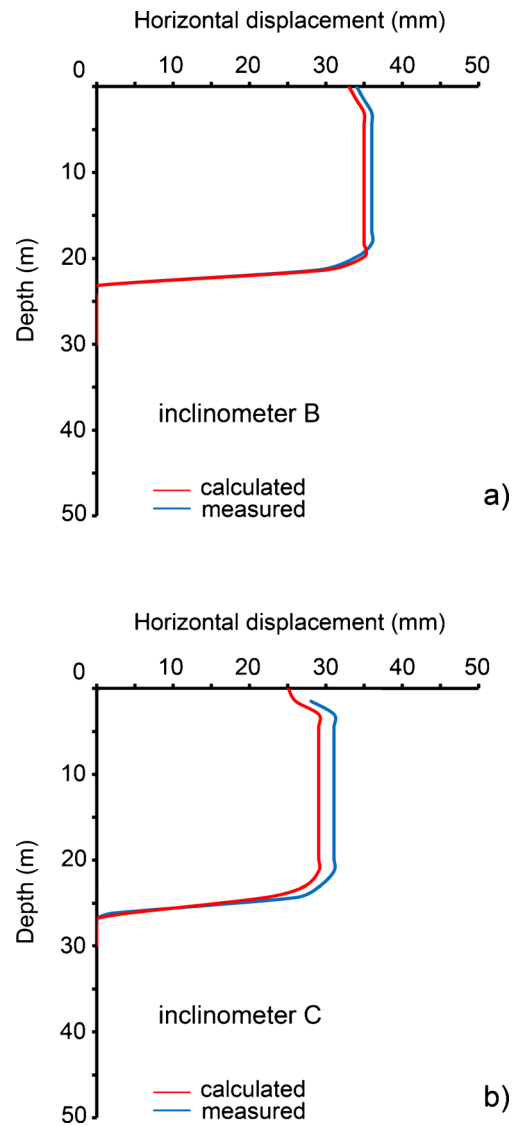


**Fig. 9** Observed and calculated displacement profiles at the inclinometers: a) B; and b) C (modified after Bertini et al. 1984)

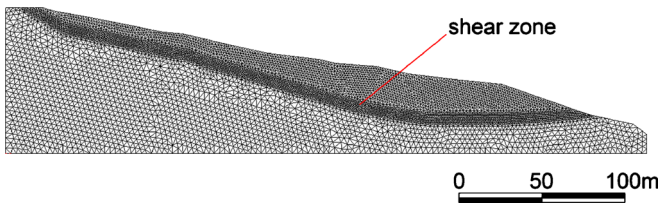


**Fig. 10** Finite element mesh used for the analysis of the Fosso San Martino landslide. The scale is applicable to the vertical and horizontal directions

response of the landslide body to groundwater fluctuations can be considered immediate. Location and thickness of the shear zones are established from the inclinometer profiles which also document the progress of horizontal displacement with time at different locations. Groundwater level measurements are also available for a sufficiently long period of observation. These monitoring data are used to validate the proposed approach and to calibrate the required soil parameters which cannot be found in the above-mentioned original studies.

The analyses were performed by the finite element code Tochnog (Roddeman 2013) in which the constitutive model described in the previous section is implemented. These analyses also accounted for the effect of hydro-mechanical coupling. The mesh adopted in the calculations consists of triangular elements with three nodes and one Gauss point. The base of the mesh is assumed to be fully impervious and fixed, and the lateral sides are constrained by vertical rollers. A hydraulic head is also imposed at the lateral boundaries. This head is governed by the measurements performed at the piezometer close to the upstream boundary or by the water level of a stream at the slope foot. Considering the uncertainties for defining the geologic history of the site and the lack of specific geotechnical data, the initial stress state within the slope is reproduced by increasing progressively the gravity acceleration up to  $9.81 \text{ m/s}^2$  (gravity loading) under the assumption that the soil in the shear zone behaves as an elastic-perfectly plastic material with Mohr-Coulomb failure criterion. The behaviour of the other involved soils is assumed elastic. At the end of the gravity loading, the associated displacements and strains are reset to zero. Then, the groundwater fluctuations measured at the piezometers installed in the slope are imposed to calculate the associated movement of the landslide. In this connection, the proposed elasto-viscoplastic constitutive model is used to simulate the behaviour of the soil in the shear zone where the deformations essentially concentrated. For the soils outside the shear zone which

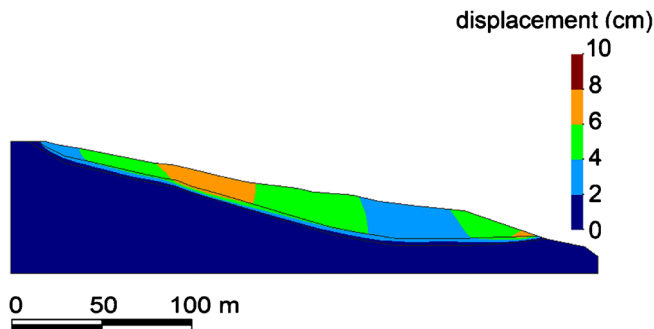


**Fig. 11** Fosso San Martino landslide: total displacement field calculated at the final time of analysis. The scale is applicable to the vertical and horizontal directions

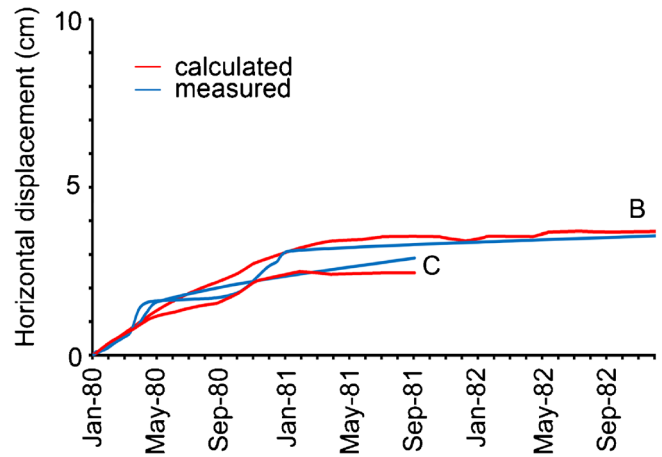


**Fig. 12** Observed and calculated horizontal displacement versus time at the top of inclinometers B and C (modified after Bertini et al. 1984)

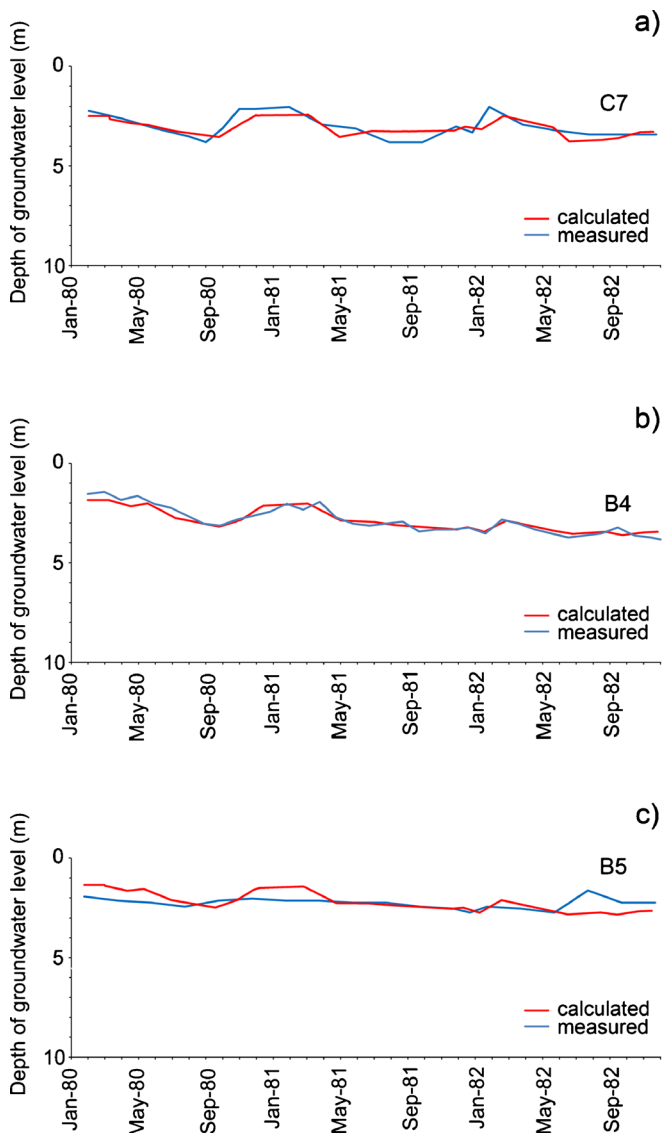


**Fig. 13** Observed and calculated piezometric levels at the piezometric cells: a) C7; b) B4; and c) B5 (modified after Bertini et al. 1984)

**Table 3** Calibrated values of the soil parameters for the Fosso San Martino landslide

Material	$\gamma$ (kN/m <sup>3</sup> )	$E'$ (MPa)	$\nu'$	$\phi_r'$ (°)	$\bar{\gamma}$ (1/day)	$k_x$ (m/day)	$k_y$ (m/day)
Colluvial cover	20.5	70	0.35			0.05	0.05
Weathered marly clay	20.5	15	0.40	16.5	$10^{-8}$	0.05	0.05
Bedrock	20.5	100	0.45			0.3	0.01

generally experienced very small deformations, an elastic model is adopted for the sake of simplicity. Considering that in the case studies analysed the water table was near the ground surface, the effect of partial saturation on the soil properties in the portion of the slope above the water table is ignored. In addition, for each case study considered, a part of the soil parameters used in the analyses derives from the field and laboratory tests conducted in the original works (Bertini et al. 1984; Corominas et al. 2005; Laloui et al. 2009). The parameters which cannot be found in these works are evaluated in the present study by matching the available monitoring data with those obtained from the numerical simulations, on a trial and error basis. The parameters resulting from this calibration could be used to predict future movements of the landslide body owing to expected groundwater fluctuations.

#### Vallcebre landslide

The Vallcebre landslide is a slow-moving translational slide affecting an area of about 0.8 km<sup>2</sup> in the Eastern Pyrenees, 140 km north of Barcelona in Spain (Corominas et al. 2005). Figure 1 shows a geological cross-section of the slope where two slide units are indicated: the intermediate unit and the lower unit. This latter is the most active slide (Corominas et al. 2005). The subsoil of the lower unit consists of a thick layer of clayey siltstone with inclusions of gypsum and fissured shale resting on a formation of limestone (bedrock). Gypsum is affected by solution processes which cause the formation of fissures, cracks and vertical cylindrical holes (pipes). A layer of fissured shale is interbedded between the layer of clayey siltstone and the bedrock. The thickness of this latter layer is about 5 m. A similar stratigraphic profile was found for the intermediate unit which is however covered by a layer of colluvial debris unlike the lower unit. A complete description of the site from a geological viewpoint can be found in Corominas et al. (2005).

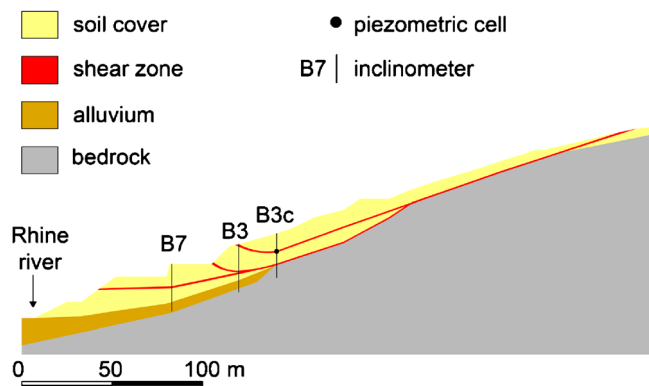


**Fig. 14** A geological cross-section of the Steinernase landslide (modified after Laloui et al. 2009). The scale is applicable to the vertical and horizontal directions

The Vallcebre landslide was monitored by installing a significant number of piezometers, inclinometers and wire extensometers. Since November 1996, systematic measurements of groundwater level and displacement of the landslide body were performed every 20 min (Corominas et al. 2005). The monitoring data showed that there is a close relationship among rainfall, groundwater fluctuations and displacement rate. In this connection, Fig. 2 relates rainfall to the available piezometric measurements, and Fig. 3 shows the piezometric levels and the landslide velocity recorded at borehole S2 (the location of which is indicated in Fig. 1) from November 1996 to October 1998. An evident synchronism exists among these records. This should be ascribed to the presence of preferential drainage ways in the upper soil layers, such as fissures, cracks and pipes, which make the response of the slope to rain infiltration practically immediate. The piezometric measurements plotted in Fig. 2 are used in the present study as input for predicting the mobility of the Vallcebre landslide.

The thickness of the lower slide unit ranges from 10 to 15 m, whereas that of the intermediate unit reaches about 34 m. Displacement occurs in a shear zone which largely develops in the layer of fissured shale (Fig. 1). At the extremities of the landslide body, the shear zone also involves the clayey siltstone formation. By contrast, deformation of the upper layers of clayey siltstone and colluvial debris is negligible (Corominas et al. 2005). Many laboratory tests were conducted to obtain the shear

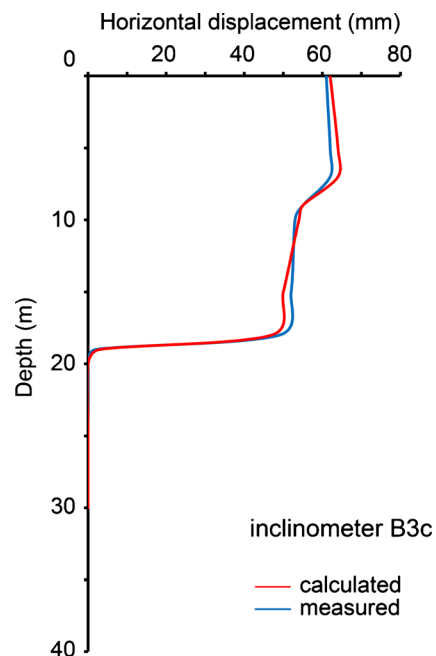


**Fig. 15** Observed and calculated inclinometric profile at borehole B3c (modified after Ferrari et al. 2008)

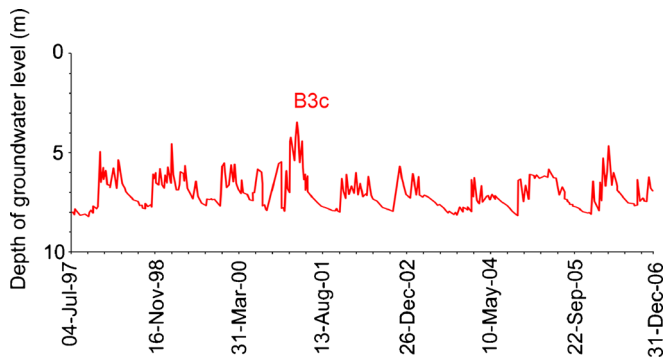


**Fig. 16** Piezometric levels measured at borehole B3c (modified after Laloui et al. 2009)

strength parameters of the soils involved by the landslide. The results from these tests can be found in the original paper by

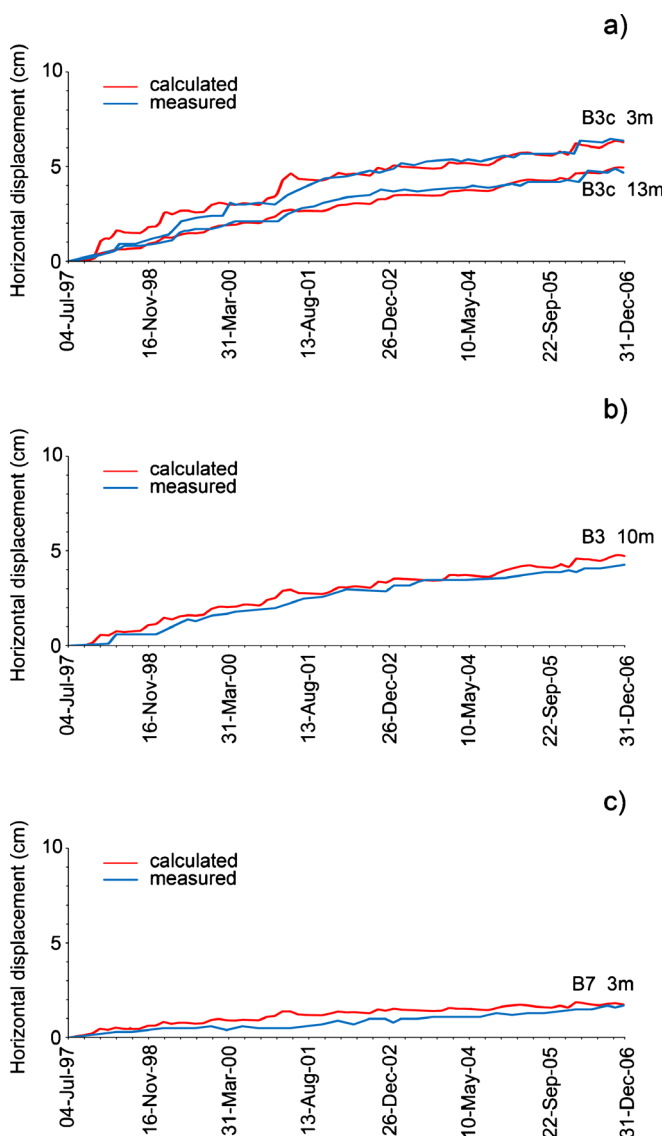


**Fig. 17** Observed and calculated horizontal displacement versus time at different depths of the boreholes: a B3c; b B3; and c B7 (modified after Ferrari et al. 2008; Laloui et al. 2009)

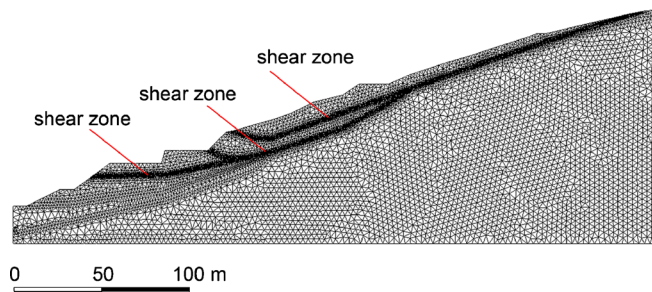


**Fig. 18** Finite element mesh used for the analysis of the Steinernase landslide. The scale is applicable to the vertical and horizontal directions

Corominas et al. (2005). In addition, some direct shear tests were performed on pre-existing shear surfaces observed in the fissured shale, from which a friction angle of  $7.8^\circ$  and an effective cohesion equal to zero were obtained. These parameters should characterise the residual shear strength of the fissured shale. In addition, it can be assumed that the residual friction angle of the clayey siltstone (in the shear zone at the extremities of the landslide body) is  $14.7^\circ$ , and the cohesion is nil (Corominas et al. 2005). The unit weight,  $\gamma$ , and the hydraulic conductivity,  $k$ , of the soils range from 20 to 22 kN/m<sup>3</sup>, and from  $10^{-9}$  to  $10^{-11}$  m/s, respectively. The other required parameters (i.e. the elastic parameters  $E'$  and  $\nu'$ , and the viscous parameter  $\bar{\gamma}$ ) are evaluated by matching the measured landslide displacements to those calculated using the present approach along with the mesh shown in Fig. 4. Considering that no inclinometric profile was shown by Corominas et al. (2005), the shear zone is simulated in the present analysis by a 1 m thick layer which is located for the most part in the fissured shales (Fig. 4). The soil of the shear zone is modelled as an elasto-viscoplastic material with residual shear strength defined by the above-specified values of  $\phi'_r$  (i.e.  $\phi'_r = 7.8^\circ$  for the portion of the shear zone located in the fissured shales and  $\phi'_r = 14.7^\circ$  for the remaining parts located in the clayey siltstone). The best agreement between measured and calculated results is achieved using the material parameters shown in Table 1. In this connection, Fig. 5 compares the accumulated displacements measured at the top of boreholes S2, S5 and S6 (see Fig. 1 for their location) with those calculated using the present approach. It is worthy to note that in this case study the updated Lagrange formulation (Roddeman 2013) was used owing to the large measured displacements. The agreement between predicted and observed movements can be on the whole considered satisfactory, although some rapid increases in displacement are not exactly reproduced in the theoretical time–displacement curves. In addition, Fig. 6 shows the total displacement field calculated at the final time of analysis. These results confirm the evidence that the lower unit is the most active slide.

#### Fosso San Martino landslide

The second case study concerns the Fosso San Martino landslide which is an active slide periodically mobilized by groundwater fluctuations, as documented by Bertini et al. (1984). This case study was analysed by several authors using different approaches (Bertini et al. 1986; D'Elia et al. 1998; Picarelli et al. 2004; Calvello et al. 2008; Conte and Troncone 2012a). The landslide is located in central Italy and is characterised by very slow movements. A representative geological cross-section of the slope is shown in

**Table 4** Calibrated values of the soil parameters for the Steinernase landslide

Material	$\gamma$ (kN/m <sup>3</sup> )	$E'$ (MPa)	$\nu'$	$\phi_r'$ (°)	$\bar{\gamma}$ (1/day)	$k$ (m/day)
Soil cover	19	15	0.40			1
Shear zone	19	10	0.40	23–27	$9 \cdot 10^{-9}$	1
Alluvium	19	200	0.40			1
Bedrock	20	500	0.40			1

Fig. 7. As it can be seen, the subsoil essentially consists of a marly clay formation (bedrock) covered by a thick layer of clayey silt (colluvial cover). The shear zone is located immediately below the colluvial cover at an average depth of about 20 m, and it involves a weathered marly clay layer the thickness of which varies from 2 to 5 m (Bertini et al. 1986; Calvello et al. 2008). Table 2 reports the available soil parameters which were obtained from laboratory and field tests by Bertini et al. (1984). In this table,  $k_x$  and  $k_y$  are the hydraulic conductivities in the horizontal and vertical directions, respectively. Several piezometric cells and inclinometers were installed within the slope. Their location is indicated in Fig. 7. The piezometric levels measured from 1980 to 1982 at the cells located close to the ground surface (Fig. 8) are used in the present study to describe the groundwater fluctuations which were responsible of the landslide mobility in the above-mentioned period of observation. In addition, Fig. 9a and b show the displacement profile at the inclinometers B and C which were installed in the central part and near the foot of the slope, respectively. These profiles reveal that the landslide body slides over the bedrock with the overlying soils that are affected by deformations of no great concern.

The mesh adopted in the calculations is shown in Fig. 10 where the shear zone is also indicated. The calculated displacement field (Fig. 11) shows the main features of the landslide kinematics. Some comparisons between measured and calculated results are presented in Figs. 9a, b and 12 in terms of displacement profiles for the inclinometers B (Fig. 9a) and C (Fig. 9b) at the final time of observation, and in terms of horizontal displacement versus time at the top of the same inclinometers (Fig. 12). In addition, Fig. 13 shows a comparison between recorded and computed piezometric levels at some cells located at different depths within the slope. As can be seen, there is a fairly good agreement between experimental and theoretical results. All these results were obtained using the

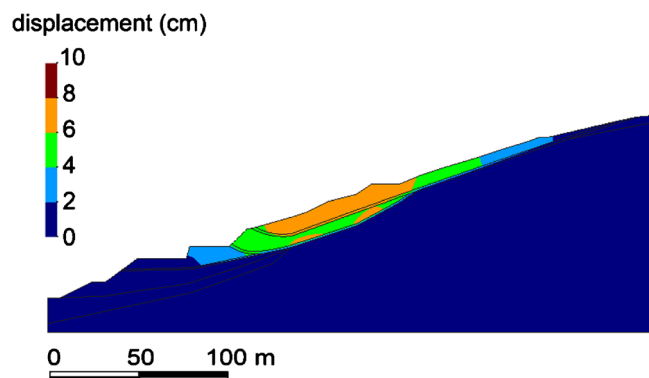


**Fig. 19** Steinernase landslide: total displacement field calculated at the final time of analysis. The scale is applicable to the vertical and horizontal directions

soil parameters indicated in Table 3, the most part of which falls in the range of the experimental values shown in Table 2.

#### Steinernase landslide

The last case study concerns the Steinernase landslide which is a slide located in the canton of Aargau, in Switzerland (Laloui et al. 2009). Pore water pressure change owing to groundwater fluctuations within the slope was recognised as the main cause for the reactivation of this landslide. A representative geological cross-section of the slope is presented in Fig. 14, from which it can be observed that the subsoil consists of an upper layer denoted as soil cover which rests on a formation of limestone (bedrock). The soil cover is principally composed of colluvial clay with a deposit of alluvium from the Rhine River at the foot of the slope. Three shear zones are also indicated in Fig. 14. Their location was carefully reconstructed on the basis of the displacement profiles recorded at the inclinometers installed in the slope. The shear zones completely develop in the soil cover and give rise to a multiple surface failure mechanism (Ferrari et al. 2008). In this connection, the inclinometric profile observed in December 2006 at borehole B3c is shown in Fig. 15 as an example. Two well-defined shear zones can be distinguished from this profile. Direct shear tests performed on specimens from the shear zones provided values of the friction angle ranging from 24° to 27° and an effective cohesion close to zero. Slightly lower values were found by Laloui et al. (2009) for the soil in the most superficial shear zone. On the basis of these data, the values of the soil friction angle assumed in the present analysis are 23°, 26° and 27° for the upper shear zone, the intermediate shear zone and the lower shear zone (Fig. 14), respectively.

Figures 16 to 17c show the piezometric levels measured from July 1997 to December 2006 at a depth of 10 m of borehole B3c (Fig. 16), and the horizontal displacements recorded at different depths of boreholes B3c (Fig. 17a), B3 (Fig. 17b) and B7 (Fig. 17c) during the same period of observation. For the sake of comparison, Fig. 17a, b and c also shows the horizontal displacements calculated using the proposed approach with the mesh shown in Fig. 18 and the soil parameters indicated in Table 4. An additional comparison in terms of displacement profile is presented in Fig. 15. As it can be seen, the finite element results compare reasonably well with the measured displacements. In addition, the calculated displacement field (Fig. 19) accounts for the multi-surface failure mechanism documented by the inclinometer profiles.

#### Concluding remarks

A finite element approach has been presented to evaluate the mobility of active slow-moving landslides owing to groundwater fluctuations. This approach includes an elasto-viscoplastic constitutive model which is used in the present study to model the



behaviour of the soil in the shear zone. For the other soils involved by the landslide, an elastic model is assumed for the sake of simplicity. Few parameters are required as input data, the most of which can be readily obtained by conventional geotechnical tests. The rest of the required parameters (in particular, the viscous parameter  $\bar{\gamma}$ ) should be calibrated on the basis of field measurements concerning the change in the groundwater levels and the associated movements of the landslide body. After being calibrated and validated, the proposed approach can be applied to situations similar to those considered in the present study to predict future landslide movements owing to expected groundwater fluctuations or to assess the effectiveness of drainage systems used as a preventive measure to control the landslide mobility.

## References

- Angeli MG, Gasparetto P, Menotti RM, Pasuto A, Silvano S (1996) A visco-plastic model for slope analysis applied to a mudslide in Cortina d'Ampezzo, Italy. *Q J Eng Geol* 29(3):233–240
- Bertini T, D'Elia B, Grisolia M, Olivero S, Rossi-Doria M (1984) Climatic conditions and slow movements of colluvium covers in central Italy. *Proc 4th Int Symp Landslides Toronto* 1:367–376
- Bertini T, Cugusi F, D'Elia B, Rossi-Doria M (1986) Lenti movimenti di versante nell'Abruzzo adriatico: caratteri e criteri di stabilizzazione. *Proc 16th Convegno Nazionale Geotecnica Bologna* 1:91–100
- Bracegirdle A, Vaughan PR, High DW (1992) Displacement prediction using rate effects on residual shear strength. *Proc 6th Int Symp Landslides Christchurch N Z* 1:343–348
- Calvello M, Cascini L, Sorbino G (2008) A numerical procedure for predicting rainfall-induced movements of active landslides along pre-existing slip surfaces. *Int J Numer Anal Methods Geomech* 32(4):327–351
- Conte E, Troncone A (2008) Soil layer response to pore pressure variations at the boundary. *Geotechnique* 58(1):37–44
- Conte E, Troncone A (2011) An analytical method for predicting the mobility of slow-moving landslides owing to groundwater fluctuations. *J Geotech Geoenviron Eng ASCE* 137(8):777–784
- Conte E, Troncone A (2012a) Stability analysis of infinite clayey slopes subjected to pore pressure changes. *Geotechnique* 62(1):87–91
- Conte E, Troncone A (2012b) Simplified approach for the analysis of rainfall-induced landslides. *J Geotech Geoenviron Eng ASCE* 138(3):398–406
- Conte E, Silvestri F, Troncone A (2010) Stability analysis of slopes in soils with strain-softening behaviour. *Comput Geotech* 37:710–722
- Corominas J, Moya J, Ledesma A, Lloret A, Gili JA (2005) Prediction of ground displacements and velocities from groundwater level changes at the Vallcebre landslide (Eastern Pyrenees, Spain). *Landslides* 2(2):83–96
- Cruden DM, Varnes DJ (1996) Landslides—investigation and mitigation. Special Report No. 247, Transportation Research Board, National Academy Press, Washington
- D'Elia B, Picarelli L, Leroueil S, Vaunat J (1998) Geotechnical characterisation of slope movements in structurally complex clay soils and stiff jointed clays. *Riv Ital Geotecnica* 32(3):5–32
- Desai CS, Samtani NC, Vulliet L (1995) Constitutive modeling and analysis of creeping soils. *J Geotech Eng ASCE* 121(1):43–56
- di Prisco C, Imposimato S (1996) Time dependent mechanical behaviour of loose sands. *Mech Cohesive-Frictional Mater* 1(1):45–73
- di Prisco C, Imposimato S (2002) Static liquefaction of a saturated loose sand stratum. *Int J Solids Struct* 39:3523–3541
- di Prisco C, Imposimato S (2003) Non local numerical analyses of strain localisation in dense sand. *Math Comput Model* 37(5–6):497–506
- Ferrari A, Laloui L, Bonnard C (2008) Case histories: geomaterial modelling of a natural slope affected by multiple slip surface failure mechanism. Intensive Course on Landslide Quantitative Risk Assessment and Risk Management, Barcelona, Spain
- Fredlund DG, Rahardjo H (1993) Soil mechanics for unsaturated soils. Wiley, New York
- Gottardi G, Butterfield R (2001) Modelling ten years of downhill creep data. *Proc 5th Int Conf Soil Mech Geotech Eng Istanbul Turk* 1–3:27–31
- Herrera G, Fernández-Merodo JA, Mulas J, Pastor M, Luzi G, Monserrat OA (2009) Landslide forecasting model using ground based SAR data: the Portalet case study. *Eng Geol* 105(3–4):220–230
- Laloui L, Ferrari A, Bonnard C (2009) Geomechanical modelling of the Steinernase landslide (Switzerland). *Proc 1st Ital Worksh Landslides Napoli* 1:186–195
- Ledesma A, Corominas J, Gonzales A, Ferrari A (2009) Modelling slow moving landslides controlled by rainfall. *Proc 1st Ital Work Landslides Napoli* 1:196–205
- Leroueil S, Vaunat J, Picarelli L, Locat J, Faure R, Lee H (1996) A geotechnical characterization of slope movements. *Proc 7th Int Symp Landslides Trondheim* 1:53–74
- Lollino P, Elia G, Cotecchia F, Mitaritonna G (2010) Analysis of landslide reactivation mechanisms in Daunia clay slopes by means of limit equilibrium and FEM methods. *Geotech Spec Publ* 199:3155–3164
- Maugeri M, Motta E, Raciti E (2006) Mathematical modelling of the landslide occurred at Gagliano Castelfranco (Italy). *Nat Hazards Earth Syst Sci* 6:133–143
- Newmark NM (1965) Effects of earthquakes on dams and embankments. *Geotechnique* 15(2):139–159
- Olivella S, Gens A, Carrera J, Alonso EE (1996) Numerical formulation for a simulator (CODE\_BRIGHT) for the coupled analysis of saline media. *Eng Comput* 13:87–112
- Perzyna P (1963) The constitutive equations for rate sensitive plastic materials. *Quart Appl Math* 20:321–332
- Picarelli L, Urciuoli G, Russo C (2004) Effect of groundwater regime on the behaviour of clayey slopes. *Can Geotech J* 41:467–484
- Roddeman D G (2013) TOCHNOG user's manual, FEAT, The Netherlands. [www.feat.nl/manuals/user/user.html](http://www.feat.nl/manuals/user/user.html)
- Savage WZ, Chleborad AF (1982) A model for creeping flow in landslides. *Bull Assoc Eng Geol* 4:333–338
- Singh A, Mitchel JK (1969) Creep potential and creep rupture of soils. *Proc 7th Int Conf Soil Mech Found Eng Mexico City* 1:379–384
- Troncone A (2005) Numerical analysis of a landslide in soils with strain-softening behaviour. *Geotechnique* 55(8):585–596
- Van Asch TWJ, Van Genuchten PMB (1990) A comparison between theoretical and measured creep profiles of landslides. *Geomorphology* 3:45–55
- Van Asch TWJ, Van Beek LPH, Bogaard TA (2007) Problems in predicting the mobility of slow-moving landslides. *Eng Geol* 91:46–55
- Vulliet L, Hutter K (1988) Viscous-type sliding laws for landslides. *Can Geotech J* 25(3):467–477

**E. Conte · A. Donato · A. Troncone** (✉)

Department of Civil Engineering,  
University of Calabria,  
Rende (Cosenza), Italy  
e-mail: antonello.troncone@unical.it

**E. Conte**  
e-mail: enrico.conte@unical.it

**A. Donato**  
e-mail: antonio.donato@nical.it